Letter of Intent to host Miniball at RIBF

N. Aoi[1], H. Baba[2], A. Blazhev[3], F. Browne[2], C. Campbell[4], M. Carpenter[5], A. Corsi[6], M.L. Cortés[2], H. Crawford[4], M. Cromaz[4], P. Doornenbal[2], P. Fallon[4], A. Gillibert[6], H. Hess[3], E. Ideguchi[1], T. Isobe[2], J. Jolie[3], V. Lapoux[6], H. Liu[8], A. Macchiavelli[4], O. Möller[8], M. Niikura[7], S. Nishimura[2], A. Obertelli[8], V. Panin[6], N. Pietralla[8], P. Reiter[3], L. Riley[9], H. Sakurai[2,7], M. Seidlitz[3], D. Suzuki[2], S. Thiel[3], V. Werner[8], N. Warr[3], K. Wimmer[7,2] and Y. Yamamoto[1]

[1]Research Center for Nuclear Physics, Osaka University, Osaka, Japan
[2]RIKEN Nishina Center, Wako, Japan
[3]Institut für Kernphysik, Universität zu Köln, Cologne, Germany
[4]Nuclear Science Division, Lawrence Berkeley National Laboratory, Berkeley, USA
[5]Physics Division, Argonne National Laboratory, Argonne, USA
[6]CEA, Centre de Saclay, Gif-sur-Yvette, France
[7]Department of Physics, University of Tokyo, Tokyo, Japan
[8]Institut für Kernphysik, Technische Universität Darmstadt, Darmstadt, Germany
[9]Department of Physics and Astronomy, Ursinus College, Collegeville, USA

November 27, 2018

1 Introduction

Since its first beam in 2006, the Radioactive Isotope Beam Factory (RIBF) of the RIKEN Nishina Center (RNC) provides highest intensity primary beams at 345 MeV/u. The great potential of the facility is best demonstrated by the search and discovery of more than 100 new isotopes [1, 2, 3, 4, 5, 6] using intense primary beams at the fragment separator BigRIPS [7]. In addition to ^{238}U, primary beams at the RIBF include ^{18}O, ^{48}Ca, ^{70}Zn, ^{124}Xe, and ^{78}Kr. In-beam γ-ray spectroscopy experiments using secondary beams typically employ the ZeroDegree spectrometer [7] for reaction product identification and the DALI2 NaI(Tl) scintillator array [8] for γ-ray detection. Owing to the high secondary beam intensities as well as detection efficiency, experiments performed at the RIBF with the most exotic nuclei are feasible nowhere else in the world. Notable examples of the RIBF's

capabilities include the first γ-ray spectroscopy of ^{54}Ca [9], ^{78}Ni [10], and ^{70}Kr [11]. Overall, in-beam γ-ray experiments currently account for about 40 % of the physics publications from NP-PAC approved experiments at the RIBF with fast radioactive beams. A complete list of obtained results to date can be found on the SUNFLOWER web-page [12].

So far, spectroscopic experiments have been largely limited to even-even nuclei in the vicinity of shell closures. Using a germanium based γ-detector will significantly enhance the capabilities of the RIBF facility and open new possibilities for experiments. Spectroscopic studies of nuclei with higher level density and lifetime measurements by Doppler-shift techniques will become possible. This Letter of Intent proposes to combine the Miniball array [13] with the BigRIPS fragment separator and the ZeroDegree spectrometer. This combination of the worlds highest secondary beam intensities with a Ge based γ-ray spectrometer will provide unique opportunities for nuclear structure as well as nuclear astrophysics studies.

2 Physics case

The RIBF provides currently worldwide uniquely high secondary beam intensities at intermediate energies ranging from 100 to 300 MeV/u. The proposed addition of the high resolution Ge-based γ-ray spectrometer Miniball will allow to access the most exotic nuclei and thus unprecedented science. Unique to the RIBF is the availability of a high intensity ^{238}U beam, giving access to the most neutron-rich nuclei around ^{78}Ni as well as heavier nuclei beyond ^{132}Sn, which are of importance for the astrophysical r-process [14]. γ-ray spectroscopy experiments in this region of the nuclear chart can to date only be performed at the RIBF.

Shell evolution towards the drip-lines, new magic numbers

Neutron-rich nuclei below ^{78}Ni display many interesting features: Halo systems have now been suggested at $N \sim 20$ [15], while the classic shell gaps $N = 20, 28$ disappear for neutron-rich nuclei resulting in a large region of deformation [16, 17]. Lifetime measurements for excited states in suggested halo nuclei would provide an independent measure of the $L = 1$ character through large $M1$ and $E2$ transitions. Tracking the evolution of the neutron $f_{7/2}$ and $p_{3/2}$ from $N = 20$ to 28 requires detailed spectroscopy of the even-odd nuclei. So far, this has only been accomplished for the Si isotopes [18] up to $N = 26$. Neutron knockout reactions with Ne or Mg isotopes would particularly benefit from the improved resolving power of Miniball compared to DALI2.

In the calcium isotopic chain two new sub-shell closures have been established experimentally at $N = 32, 34$ [9, 19, 20]. Theoretical calculations [21] show that three-nucleon forces play an important role in the microscopic description of these nuclei. Spectroscopy of Ca isotopes at RIBF has recently been extended to $N = 36$ for 2^+_1 states and single-particle properties studied in the neutron and proton removal reactions from ^{54}Ca within the SEASTAR project [22]. Beyond Ca, the Ti isotopes show a staggering of collectivity which is not yet understood in either beyond mean field [23] as well as shell model [24] calculations. Lifetime measurements beyond the 2^+ states, states in the odd-N Ca and Ti isotopes, as well as spectroscopic factors obtained from knockout reactions will provide more stringent tests of the robustness of the closed-shell cores and the role of three-body forces for non-magic isotopes. Generally, due to the onset of collectivity and complexity of the level structures, odd-even nuclei beyond $Z = 20$ have been challenging with DALI2, as seen already for ^{55}Sc [25]. An abundance of new spectroscopic details may be revealed by utilizing Miniball.

Collectivity and breakdown of the harmonic oscillator shell closure at $N = 40$ has been established through measurements of collective properties, excitation energies, and level lifetimes (see for example Refs. [26, 27, 28] for most recent experimental data). A new island of inversion has been predicted with a center at ^{64}Cr [29]. Experimental data on spin and parity assignments as well as level occupations is sparse in the region of neutron-rich $N = 40$ nuclei. High-resolution spectroscopy of the even-odd nuclei ^{67,69}Fe, ^{63,65}Cr, and ^{57,59}Ti from one-neutron knockout reactions will fill this gap and reveal whether its inversion extends down towards ^{60}Ca.

Excited states in ^{78}Ni and ^{79}Cu have recently been studied at the RIBF facility with a high intensity ^{238}U primary beam [10, 30]. Tracking the evolution of the shell gaps along $N = 50$ and $Z = 28$ as predicted in Ref. [31] requires precise measurements of odd nuclei through knockout reactions. Lifetime measurements of neutron-rich Zn, Ge, and Se nuclei with $N > 50$ to delineate the onset of collectivity beyond ^{78}Ni will be possible as well.

Lifetime measurements and spectroscopy of odd-A nuclei in the region of doubly-magic ^{132}Sn will provide constraints for shell model calculations in the region south-east of ^{132}Sn where spectroscopy so far is sparse. This region is extremely important to understand nucleo-synthesis in the r-process and shell evolution in heavy nuclei. The filling of the $2f_{7/2}$ orbital in Sn isotopes beyond ^{132}Sn resembles the situation in the Ca isotopes, and a new magic number is predicted at $N = 90$ [32], but precise single particle spectroscopy and their evolution along the Sn isotopic chain beyond $N = 83$ are not yet available from experiment.

$N = Z$: the rp-process, mirror symmetry, and the quest for ^{100}Sn

Along the $N = Z$ line of the nuclear chart, a number of interesting physics cases can be studied. Proton-rich nuclei along $N = Z$ constitute the path of the rapid proton-capture process (rp-process), that powers type I X-ray bursts. While direct measurements of (p, γ) reaction rates on these radioactive isotopes are not feasible in all cases, indirect measurements of excited states in the final nuclei as well as spectroscopic factors from (d,n) reactions can significantly reduce the uncertainties associated with the calculation of element abundances in the rp-process [33].

$N \sim Z$ nuclei also provide an interesting testing ground to investigate the breaking of charge symmetry and charge independence. Measurements of Coulomb energy and mirror energy differences have been limited so far to $A = 70$ and low spin values [34, 11]. Data for higher (medium) spin values and odd-even nuclei are required to clarify the role of isospin-non-conserving forces and neutron skin effects [35]. The high intensity ^{78}Kr and ^{124}Xe primary beams at RIBF combined with the high in-beam energy resolution of Miniball allow for detailed spectroscopy of nuclei between $A = 50$ and 100. In addition to nuclear structure information, new data on waiting point nuclei of the rp-process predicted in this region can be obtained.

The region around ^{100}Sn has attracted a lot of interest. B(E2) values in light tin isotopes are larger than expected [36, 37], and the ordering of the neutron $\nu g_{7/2}$ and $\nu d_{5/2}$ orbitals above $N = 50$ seems to be inverted [38]. Spectroscopy of ^{101,103}Sn and ^{101,103}In through proton or neutron knockout and well as (p, p') with the MINOS liquid hydrogen target [39] will contribute to the understanding of unexpected high collectivity in the light even-even Sn nuclei.

Shape evolution and coexistence around $A \sim 100$ and in the rare earth region

Between $N = 50$ and $N = 82$, nuclei show an interesting interplay of single-particle and collective excitation modes. In the Sr and Zr isotopes, a sudden onset of collectivity at $N = 60$, which extends at least to ^{110}Zr [40], is accompanied with shape coexistence at low excitation energies [41, 42]. Detailed spectroscopy of odd-mass in this region will help unravel the orbitals involved. In contrast, for the Kr isotopes a drop in the 2^+ excitation energy associated with an onset of deformation is not observed [43, 44]. Additional information could come from lifetime measurements and off-yrast spectroscopy through secondary fragmentation reactions and spectroscopy of odd-even nuclei.

High intensity radioactive beams with $Z \gtrsim 50$ are unique to the RIBF facility. Measurements of collective properties, excited state lifetimes, and proton inelastic scattering will shed new light on the evolution of collectivity and shape coexistence in the rare earth region. Measurements of single-particle properties will give hints on the underlying microscopic structure and new constraints for astrophysical r-process calculations.

Octupole collectivity in $A \sim 90$ and 140 nuclei

In regions where neutrons and protons occupy orbitals at the Fermi surface with $\Delta j = \Delta \ell = 3$, strong octupole correlations can break the reflection symmetry of nuclei resulting in octupole deformed shapes. Octupole collectivity is expected in the Ra-Th region, and for neutron-rich

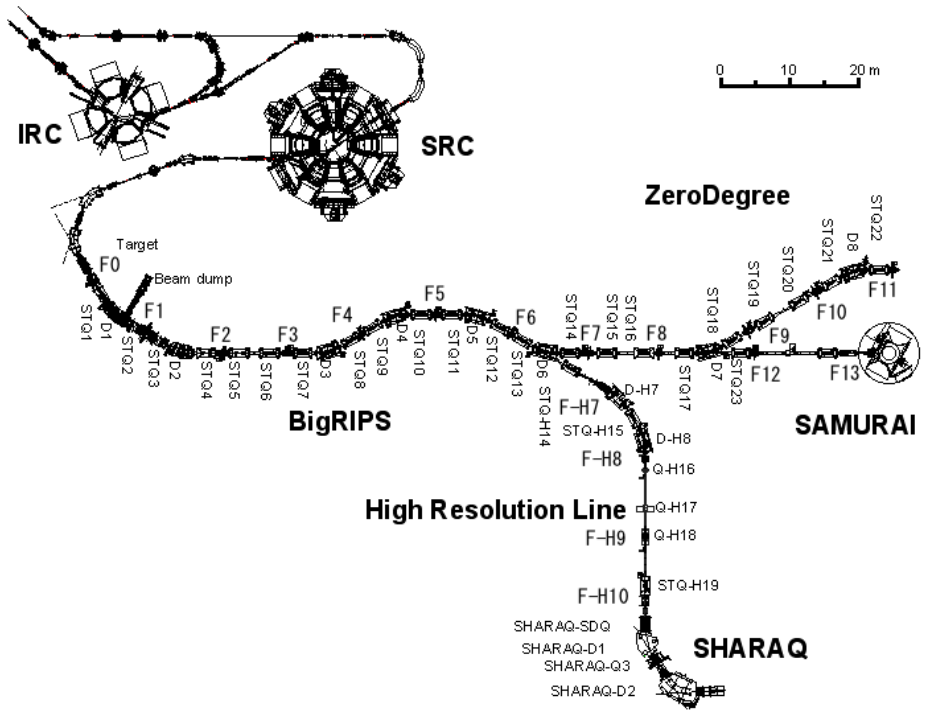

Figure 1: Overview of the RIBF facility. Not shown are the initial acceleration states. The BigRIPS fragment separator is used to purify and identify the radioactive ion beams. In-beam γ-ray spectroscopy is performed at the focal point F8. Reaction products are uniquely identified using the ZeroDegree spectrometer (F8 - F11).

nuclei in the region around ^{144}Ba [45] and ^{90}Se. In the first case, it would be interesting to see if the region of octupole deformation extends to other nuclei, i.e. Xe or Ce, or the proton-odd neighbors. $(p, 2p)$ reactions on the MINOS liquid hydrogen target [39] enable the population of excited states in this region. The combination with high-resolution γ-ray spectroscopy opens, for the first time, also access to odd isotopes. Moreover, such reactions will shed new light on the single-particle structures underlying the collective states. Around $A = 90$, first spectroscopy of ^{90}Se has only been performed recently [46], and information beyond the mere location of states is necessary to asses the onset of octupole deformation, for example by means of lifetime measurements.

3 In-beam γ-ray spectroscopy at the RIBF

It is proposed to couple the Miniball array with BigRIPS fragment separator and the ZeroDegree spectrometer at the RIBF. Experimental details are briefly described in the following section, highlighting the unrivaled possibilities for in-beam γ-ray spectroscopy experiments offered at the RIBF.

3.1 The RIBF facility

The facility for radioactive isotope research is schematically shown in Figure 1. Stable beams are accelerated up to 345 MeV/u using a linear accelerator followed by four cyclotrons. Primary beam intensities for this energy are summarized in Table 3.1.

beam particle	beam current [pnA] maximum	expected
^{18}O	1000	500
^{48}Ca[1]	730	500
^{70}Zn	250	200
^{78}Kr	480	300
^{124}Xe	100	80
^{238}U	58	40[2]

[1] ^{48}Ca might not be available in 2020.
[2] In fall 2018, a stable primary beam intensity of 60 pnA was maintained for ^{238}U.

Table 1: Primary beam intensities at 345 MeV/u [47] for the facility operation in FY2018. Maximum achieved and expected beam currents are given in pnA.

3.2 BigRIPS and ZeroDegree Spectrometer

Primary beams impinge on the production target (F0); their fragmentation or fission products are subsequently separated in the two-stage separator BigRIPS. Event-by-event identification is facilitated by $B\rho$, ΔE, and time-of-flight measurements between the focal points F3 and F7. Positions and angles of beam particles are measured using parallel plate avalanche counters (PPAC), the time-of-flight is measured with plastic scintillators at F3 and F7. At F7, an ionization chamber allows for unique Z identification through an energy loss measurement. Maximum rates are several tens of kHz. The total momentum acceptance amounts to ±3 %, with a momentum resolution of 3440. A relative A/Q resolution of 0.034 % has been achieved [48], allowing for the separation of fully stripped from hydrogen-like charge states. Production cross sections of radioactive ions have been measured for a wide range of nuclei [2, 5, 6] providing validation of the theoretical fragmentation and fission cross sections employed in LISE++ simulations. Secondary beam intensities for experiments can therefore be predicted reliably, allowing for an straightforward planning of experiments at the RIBF.

In-beam γ-ray spectroscopy experiments are typically performed with thick solid secondary reaction targets (Be, C, Au, Pb, etc.) at F8 in the order of 1 g/cm^2 depending on the case of interest. The size of the beam spot on the target amounts typically to $\sigma = 5$ mm in X and Y. Tracking of the beam onto the target is facilitated by a set of two PPACs in front of the target (position resolution $\sigma = 0.7$ mm), the scattering angle can be reconstructed using a third PPAC behind the target (in front of STQ17 in Figure 1) with an accuracy of ≈5 mrad [37]. For the campaign of Miniball at the RIBF, we envision to use solid targets, the liquid hydrogen target MINOS [39], or a plunger for lifetime measurements. For experiments with solid targets, the present setup at F8 with three PPACs and a beam pipe of 150 mm diameter is used, allowing to place the γ-ray detectors close to the target to maximize the efficiency.

The ZeroDegree spectrometer is used for identification of reaction products behind the secondary target located at F8 (see Figure 1). Particle identification is obtained in an analogous way to the BigRIPS separator by using $B\rho$, ΔE, and time-of-flight measurements between F8 and F11. Typical beam energies after the target amount to $100 - 200$ MeV/u. Therefore, for high Z nuclei not all reaction products will be in the fully stripped charge state. With the high resolution for the mass to charge ratio A/Q it is possible to discriminate different charge states up to $Z \approx 55$, $A \approx 150$. Additionally, a total kinetic energy detector can be placed at the end of the beam-line after the last ionization chamber at F11. Three different optics modes are possible for the ZeroDegree spectrometer: Large acceptance, high resolution, and dispersive. With a momentum resolution of $p/\Delta p = 1240$, the large acceptance mode offers sufficient accuracy for parallel momentum distributions to deduce angular momentum L assignments.

3.3 Miniball at RIBF

In-beam γ-ray spectroscopy at the RIBF has so far been mostly restricted to the spectroscopy of even-even nuclei. Spectroscopy of odd nuclei is challenging due to the limited energy resolution, except for certain cases close to magic numbers [25, 30]. The in-beam energy resolution depends critically on the intrinsic energy as well as position resolution, as shown in Figure 2 (a).

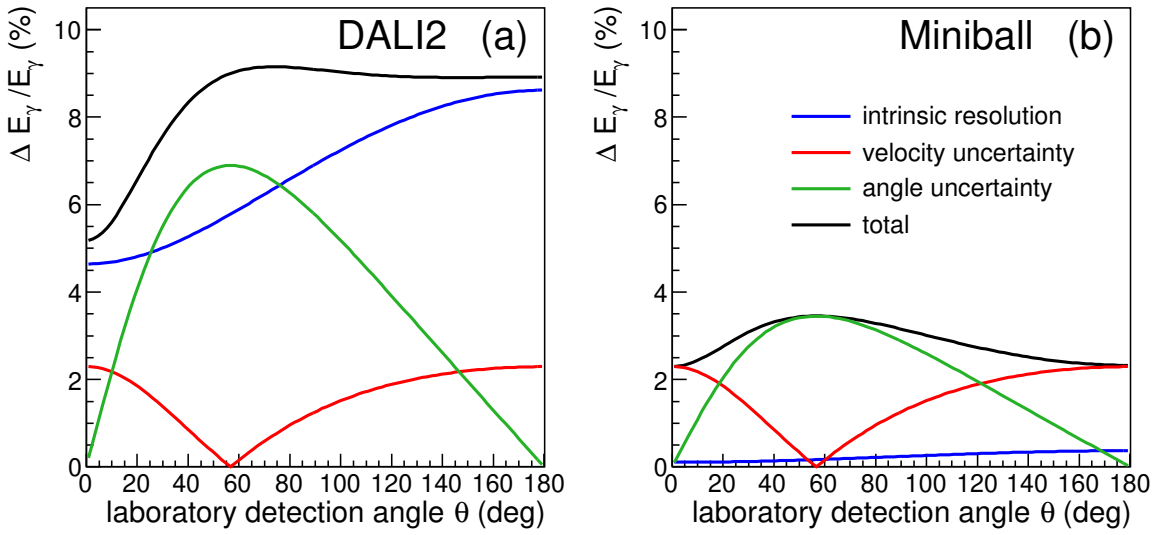

Figure 2: Energy resolution of Miniball (b) in comparison with DALI2 (a). The total in-beam energy resolution (black) depends on the intrinsic energy resolution (blue), the position resolution for the Doppler correction (green), as well as the velocity uncertainty due to the energy loss in the target (red). Uncertainties are calculated for a 200 MeV/u beam impinging on a 4 mm Be secondary target ($\langle\beta\rangle = 0.55$, $\Delta\beta = 0.016$) emitting a 1 MeV γ ray. Great improvements in the intrinsic energy as well a position resolution of Miniball compared to DALI2 allow for spectroscopy with about 2–3 % final energy resolution for in-beam experiments. Doppler correction on the segment level was assumed for this plot.

With Miniball, the obtainable energy resolution following Doppler correction depends on exact distance to the target, the energy and mass of the secondary beam, and the secondary target thickness. Figure 2 shows the parameters of a typical in-beam γ-ray experiment at the RIBF. Assuming a distance of 200 mm from the target, the resolution with Miniball is improved by a factor three compared to DALI2. For larger distances between detectors and target, better resolutions can be obtained.

The nominal efficiency of Miniball amounts to 7.8 % at 1.3 MeV [13] using add-back. For experiments at RIBF, the distance to the target is larger than for the typical experiments performed at REX-ISOLDE. Thus, a reduced efficiency is expected. For experiments with fast beams performed at GSI, the array was placed at angles of 51 and 85° at about 220 mm distance, resulting in an efficiency of 3 % at 1.3 MeV [49]. For experiments at the RIBF, we plan to install six clusters at 30° and two clusters at 65° at a distance of 200 mm from the target. The in-beam full energy peak (FEP) efficiency at 1 MeV in this case is 4.1 % and 1.1 %, respectively for the detectors at 30 and 65°. Typical resolutions are on the order of 2–3 % (FWHM) after Doppler correction, depending on the target thickness and the beam properties.

Experiments at RIBF typically involve low beam intensities. The maximum total rate at F8 is a few tens of kHz. Reactions at relativistic energies on the secondary targets produce some particle background, but the flux is low, such that there is no radiation damage of the detectors from, for example, neutrons.

3.4 Ancillary detectors

It is planned to couple Miniball to other Ge detector systems. Discussions are ongoing to use the tracking detectors from Lawrence Berkeley National Laboratory (triplet GRETINA prototype), RCNP Osaka (quad GRETINA-type), and TU Darmstadt (DAGATA triple) to maximize the efficiency and resolution. The planned configuration of the array is shown in Figure 3.

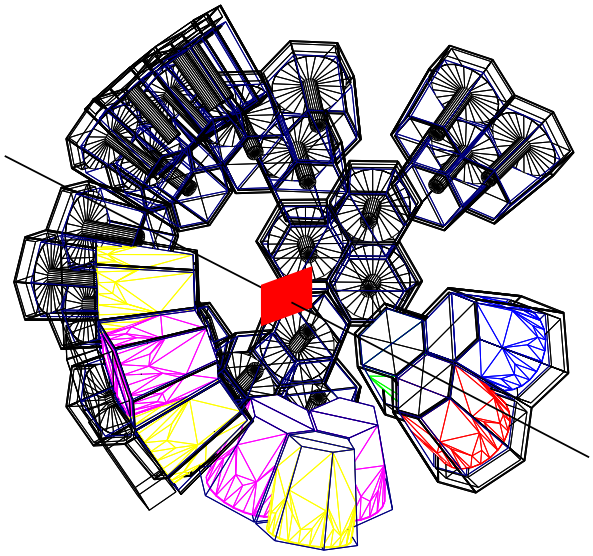

Figure 3: Setup in the simulation. The beam is coming from the lower right impinging on the target located at the center of the array. Six Miniball clusters are located at 30°, two at 65°, additional tracking γ-ray detectors are also located at 65°.

GEANT4 [50] simulations for the Miniball array in addition to the ancillary detectors were initially carried out for a 1 MeV γ ray emitted at 100 MeV/u. The in-beam resolutions amounted to $0.15 - 1.56$ % (σ) for the ideal no target case and $0.33 - 2.54$ % (σ) for a realistic reaction on a 3 mm thick Be secondary target. The total in-beam FEP efficiency amounted to 9.4 %.

4 Simulation results, expected performance

In order to estimate the performance of the proposed array combining the Miniball cluster detectors with γ-ray tracking detectors GEANT4 simulations have been carried out under experimental conditions. These included a realistic geometry of the detectors, the crystals and the cryostats, as well as the beam pipe. The reaction dynamics of knockout and inelastic scattering reactions were implemented through a parametrization of the ejectile momentum and angular distributions. In the analysis of the simulated data, the Doppler correction was performed assuming the Miniball segment with the highest energy deposition recorded the first interaction of the γ-ray. For the angle, the weighted average position of hits in the segment was used in addition to the scattering angle of the ejectile. An event-by-event mid-target velocity β was reconstructed from the ejectiles momentum distribution. Add-back analysis was performed based on the link algorithm within a clustering angle of 20°. Tracking was implemented for the ancillary detectors described above.

First spectroscopy of excited states of the $N = 50$ nucleus ^{79}Cu has been recently performed at RIBF using DALI2 [30]. With a limited intrinsic and in-beam resolution, the construction of the level scheme is largely guided by comparison to theoretical calculations. Figure 4 shows a simulation of the experiment using either DALI2 or the Ge based array using eight Miniball and three tracking clusters. The number of emitted γ rays is identical in both simulations. The improved resolution with the Ge based detectors permits unambiguous identification of faint lines in the spectrum.

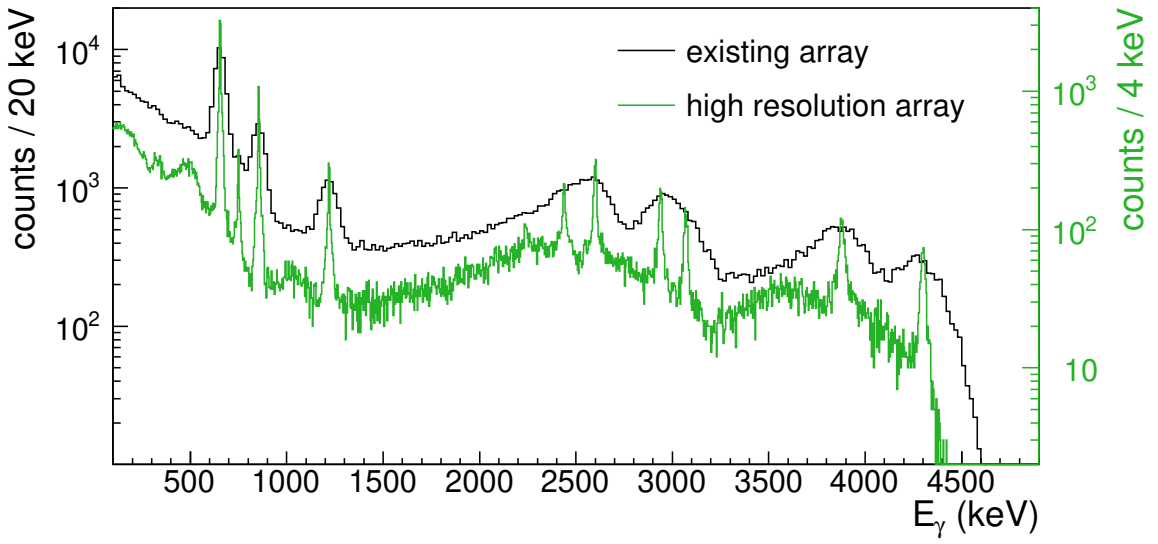

Figure 4: Simulation of the one-proton knockout reaction from ^{80}Zn to ^{79}Cu in comparison with DALI2. The simulated DALI2 data correspond to the results from a recent RIBF experiment [30].

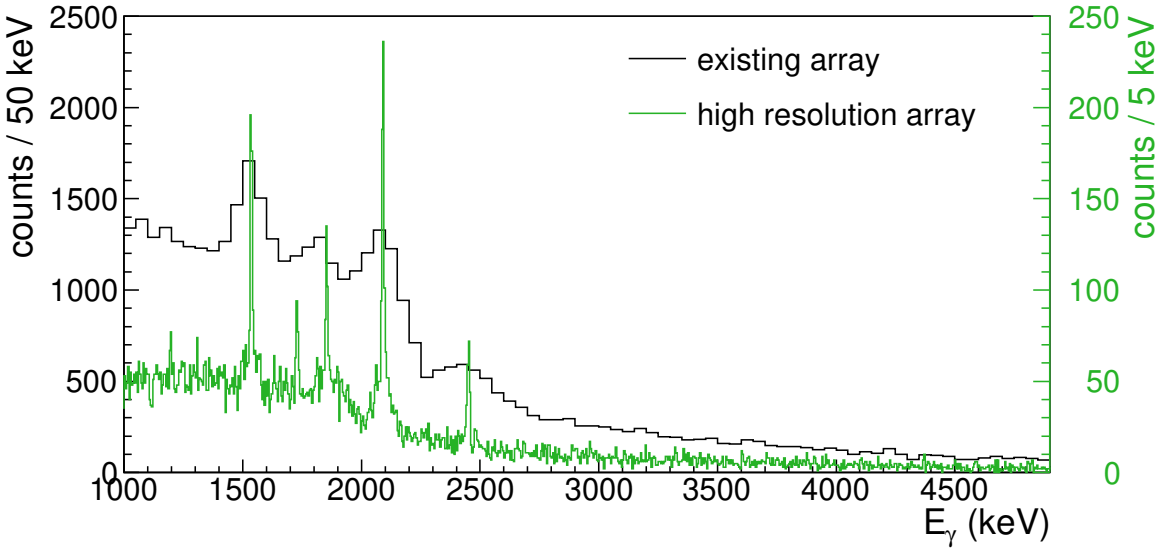

Figure 5: Simulation of the one-proton knockout reaction from ^{56}Ti to ^{55}Sc using Miniball (green) in comparison with DALI2 (black). The simulated DALI2 data correspond to the results from a recent RIBF experiment [25].

As the new $N = 34$ sub-shell closure between the neutron $2p_{1/2}$ and $1f_{5/2}$ orbitals is only observed in the Ca isotopes, and not in the heavier Ti isotopes, the intermediate isotope ^{55}Sc located in-between is of key interest. Spectroscopy of this nucleus can clarify this peculiar behavior which, so far, is not fully understood. Spectroscopy of ^{55}Sc has been performed [9] with DALI2. The comparison is shown in Figure 5. A realistic background obtained from the experiment has been implemented in the simulation. The improved resolution using high-resolution γ-ray detectors is evident, allowing for simultaneous lifetime measurements which were so far experimentally inaccessible. Furhtermore, the superb peak-to-background ratio allows for gating on individual transitions to measure final state

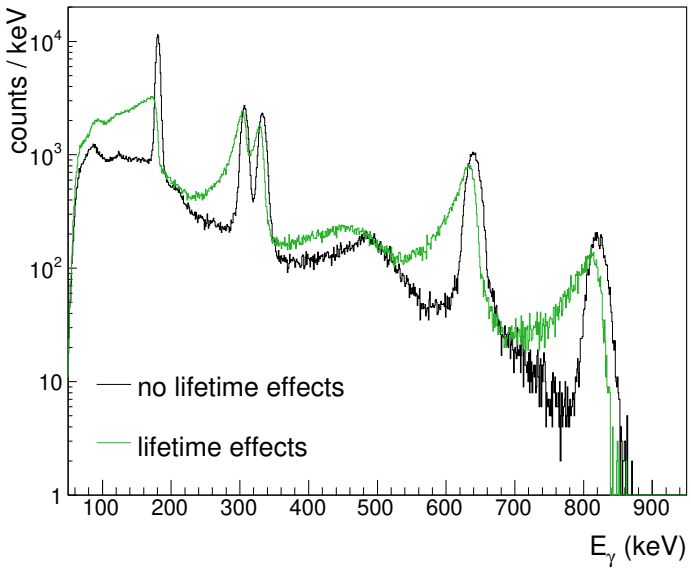

Figure 6: Simulation of lifetime effects. The decay of the 3_1^- state in ^{146}Ba to the ground state and through the 2^+ and 4^+ states has been simulated with realistic lifetimes (green) and without any lifetime effects (black).

exclusive momentum distributions and thus assign spin and parity quantum numbers to the levels populated in the knockout reaction. The narrow peak width also reduces the background in the $\gamma-\gamma$ coincidence matrix used to construct the level scheme.

In fact, the prospect to perform lifetime measurements emerges as further immense benefit of high resolution spectroscopy in combination with fast radioactive beams. This possibility is explored in Figure 6. Here, the simulation compares Coulomb excitation of ^{146}Ba with and without the well-known level lifetimes. The decay of the 3^- state with a half-life of 237 ps feeds the 2^+ and 4^+ states in addition to the ground state (821 keV transition). The 2^+ state has a long half-life of 0.859 ns, which results in a very long tail. Unknown lifetimes can be measured by comparing the measured γ-ray energy spectrum to simulations with varying lifetimes and fitting the best matching lifetime to the data [51].

5 Requested equipment, support, and maintenance

We intend to host eight Miniball triple clusters for the calendar year 2020. In addition, we require parts of the filling system and the liquid nitrogen hoses. The support structure for Miniball may be obtained from the University of Cologne.

The DGF based data-acquisition system used so far for Miniball is not needed. Instead, the data acquisition will be provided by this collaboration. Specifically, digitizers based on the GRETA design from the CAGRA project [52] will be used for the Miniball detectors. This acquisition system will be integrated in the RIBF DAQ framework and correlated with the BigRIPS and ZeroDegree systems by time-stamping or common trigger. Further funds for the digitizers and trigger modules for the ancillary detectors within the array have been requested from the Japanese Society for the Promotion of Science.

The RIBF has ample experience with hosting Ge detector arrays, for example hosting EURICA from 2012–2016 [53, 54]. Parts of the infrastructure from the EURICA campaign exists and can be used for Miniball. A reliable liquid nitrogen filling system is available and will be extended. High voltage supply, monitoring, and temperature monitoring systems as well as an uninterruptible power

supply unit will be provided by the RIBF.

Packing and transportation costs of the detectors from CERN, or elsewhere, will be provided by RIKEN. Travel and local support for members of the Miniball collaboration for dismounting at CERN and setup at RIBF will also be provided. This includes on-site maintenance during the experiment in case needed.

6 Project Time-Line

In parallel to this Letter of Intent, the collaboration has submitted a construction proposal to the next RIBF Nuclear Physics Program Advisory Committee. This construction proposal includes the ancillary detectors as well. The decision on the proposal will be made at the NP-PAC meeting in November 2018.

A dedicated workshop will be held in spring 2019, either at RIBF or in Europe, to discuss the physics proposals and details of the setup. The call for nuclear physics proposals to the NP-PAC is usually issued in July/August with a submission deadline in October 2019. This call will explicitly solicit proposals for Miniball and the ancillary devices. Application for beam time is open to all RIBF users. Beam-time will be awarded based on the recommendation by the NP-PAC committee in their meeting in December 2019. The RIBF will allocate 30 days of beam on target time for the experimental campaign in spring 2020 and further beam time in fall 2020 depending on the NP-PAC recommendation. Within these campaigns, we anticipate about 10 experiments.

References

[1] T. Ohnishi et al. *J. Phys. Soc. Jpn.*, 79:073201, 2010.

[2] H. Suzuki et al. *Nucl. Instrum. Meth. B*, 317:756, 2013.

[3] I. Celikovic et al. *Phys. Rev. Lett.*, 116:162501, 2016.

[4] O. B. Tarasov et al. *Phys. Rev. Lett.*, 121:022501, 2018.

[5] Y. Shimizu et al. *J. Phys. Soc. Jpn.*, 87:014203, 2018.

[6] N. Fukuda et al. *J. Phys. Soc. Jpn.*, 87:014202, 2018.

[7] T. Kubo et al. *Prog. Theor. Exp. Phys.*, 2012:03C003, 2012.

[8] S. Takeuchi et al. *Nucl. Instrum. Meth. A*, 763:596, 2014.

[9] D. Steppenbeck et al. *Nature*, 502:207, 2013.

[10] R. Taniuchi. PhD thesis, The University of Tokyo, 2018.

[11] K. Wimmer et al. *Physics Lett. B*, 785:441, 2018.

[12] SUNFLOWER publications. `http://www.nishina.riken.jp/collaboration/SUNFLOWER/publication/bigrips.html`, 2018.

[13] N. Warr et al. *Eur. Phys. J. A*, 49:40, 2013.

[14] G. Lorusso et al. *Phys. Rev. Lett.*, 114:192501, 2015.

[15] T. Nakamura et al. *Phys. Rev. Lett.*, 112:142501, 2014.

[16] P. Doornenbal et al. *Phys. Rev. Lett.*, 111:212502, 2013.

[17] E. Caurier et al. *Phys. Rev. C*, 90:014302, 2014.

[18] S. R. Stroberg et al. *Phys. Rev. C*, 91:041302, 2015.

[19] F. Wienholtz et al. *Nature*, 498:346, 2013.

[20] S. Michimasa et al. *Phys. Rev. Lett.*, 121:022506, 2018.

[21] J. D. Holt et al. *Phys. Rev. C*, 90:024312, 2014.

[22] SEASTAR project. `http://www.nishina.riken.jp/collaboration/SUNFLOWER/experiment/seastar/index.html`, 2018.

[23] Tomás R. Rodríguez and J. Luis Egido. *Phys. Rev. Lett.*, 99:062501, 2007.

[24] L. Coraggio et al. *Phys. Rev. C*, 89:024319, 2014.

[25] D. Steppenbeck et al. *Phys. Rev. C*, 96:064310, 2017.

[26] H. L. Crawford et al. *Phys. Rev. Lett.*, 110:242701, 2013.

[27] A. Gade et al. *Phys. Rev. Lett.*, 112:112503, 2014.

[28] C. Santamaria et al. *Phys. Rev. Lett.*, 115:192501, 2015.

[29] S. M. Lenzi et al. *Phys. Rev. C*, 82:054301, 2010.

[30] L. Olivier et al. *Phys. Rev. Lett.*, 119:192501, 2017.

[31] Y. Tsunoda et al. *Phys. Rev. C*, 89:031301, 2014.

[32] S Sarkar and M Saha Sarkar. *J. of Phys.: Conf. Ser.*, 267:012040.

[33] C. Langer et al. *Phys. Rev. Lett.*, 113:032502, 2014.

[34] A. Obertelli et al. *Physics Lett. B*, 701:417, 2011.

[35] A. Boso et al. *Phys. Rev. Lett.*, 121:032502, 2018.

[36] V. M. Bader et al. *Phys. Rev. C*, 88:051301, 2013.

[37] P. Doornenbal et al. *Phys. Rev. C*, 90:061302, 2014.

[38] I. G. Darby et al. *Phys. Rev. Lett.*, 105:162502, 2010.

[39] A. Obertelli et al. *Eur. Phys. J. A*, 50:8, 2014.

[40] N. Paul et al. *Phys. Rev. Lett.*, 118:032501, 2017.

[41] P. Federman and S. Pittel. *Phys. Rev. C*, 20:820, 1979.

[42] T. Togashi et al. *Phys. Rev. Lett.*, 117:172502, 2016.

[43] M. Albers et al. *Phys. Rev. Lett.*, 108:062701, 2012.

[44] F. Flavigny et al. *Phys. Rev. Lett.*, 118:242501, 2017.

[45] B. Bucher et al. *Phys. Rev. Lett.*, 116:112503, 2016.

[46] S. Chen et al. *Phys. Rev. C*, 95:041302, 2017.

[47] RIBF Technical Information website. `http://www.nishina.riken.jp/RIBF/accelerator/tecinfo.html`, 2018.

[48] N. Fukuda et al. *Nucl. Instrum. Meth. B*, 317:323, 2013.

[49] P. Doornenbal. PhD thesis, Universitẗ zu Köln, 2007.

[50] S. Agostinelli et al. *Nucl. Instr. Meth. A*, 506:250, 2003.

[51] A. Lemasson et al. *Phys. Rev. C*, 85:041303, 2012.

[52] CAGRA project.
`http://www.rcnp.osaka-u.ac.jp/Divisions/np1-a/CAGRA/index.html`, 2018.

[53] S. Nishimura. *Prog. Theor. Exp. Phys.*, 2012:03C003, 2012.

[54] P.A. Söderström et al. *Nucl. Instr. Meth. B*, 317:649, 2013.